

UC San Diego

UC San Diego Previously Published Works

Title

Density-dependent mortality in an oceanic copepod population

Permalink

<https://escholarship.org/uc/item/2h63s0h0>

Journal

Nature, 412(6847)

ISSN

0028-0836

Authors

Ohman, MD

Hirche, H-J

Publication Date

2001-08-01

DOI

10.1038/35088068

Peer reviewed

Cloning and sequencing

The amplified *nifH* fragments, approximately 359 base pairs in length, were cloned in Promega pGEM-T vector using the manufacturer's protocol. Recombinants containing the cloned insert were identified by restriction fragment analysis, and the fragment sequenced using an ABI 310 automated DNA sequencer. The translated sequences were aligned with Genetics Computer Group software, and the phylogenetic relationship determined by a distance method and neighbour joining using TREECON software²⁸. The analysis was bootstrapped 100 times.

Epifluorescence microscopy

Formalin-preserved water samples (10–20 ml) were filtered onto black polycarbonate Poretics filters (pore size 0.22 µm). An Olympus BX-60 epifluorescence microscope was used with the U-WMB filter set (excitation 450–480 nm; emission greater than 515 nm). Phycoerythrin-containing cells (fluorescing yellow–orange) were enumerated in 100 fields, and cells were measured using an ocular micrometer.

¹⁵N experiments

Water collected from a depth of 25 m at station ALOHA in July 2000 was transported to the marine laboratory at the Hawaii Institute of Marine Biology, where it was incubated in 2–4-l acid-washed polycarbonate bottles in running seawater, in a flume. The flume was covered with one layer of neutral-density screening to decrease light levels to roughly 50% surface irradiance (photosynthetically active radiation) approximately 600 µmol m⁻² s⁻¹). At each time point, samples were processed for ¹⁵N and microscopy, after pre-filtering through Nuclepore filters (pore size 10 µm) to remove the larger diazotrophs. Particle samples were collected by gentle pressure filtration (<10 pounds per square inch) through pre-combusted GF/F filters, which were analysed ashore by continuous-flow isotope ratio mass spectrometry using a Micromass Optima mass spectrometer that was interfaced with a CE-Elantech NA2500 elemental analyser. The analytical precision varies with sample size, but is about ± 0.2% (s.d. of replicate analyses) for samples containing 0.5–2 µmol of N.

Received 12 February; accepted 12 June 2001.

- Vitousek, P. M. & Howarth, R. W. Nitrogen limitation on land and in the sea: how can it occur? *Biogeochemistry* **13**, 87–115 (1991).
- Howarth, R. W. & Marino, R. Nitrogen fixation in freshwater, estuarine, and marine ecosystems. 2. Biogeochemical controls. *Limnol. Oceanogr.* **33**, 688–701 (1988).
- Falkowski, P. G. Evolution of the nitrogen cycle and its influence on the biological sequestration of CO₂ in the ocean. *Nature* **387**, 272–275 (1997).
- Haug, G. H. et al. Glacial/interglacial variations in production and nitrogen fixation in the Cariaco Basin during the last 580 kyr. *Paleoceanography* **13**, 427–432 (1998).
- Paerl, H. W. Physiological ecology and regulation of N₂ fixation in natural waters. *Adv. Microb. Ecol.* **8**, 305–344 (1990).
- Dugdale, R. C., Menzel, D. W. & Ryther, J. H. Nitrogen fixation in the Sargasso Sea. *Deep-Sea Res.* **7**, 298–300 (1961).
- Gruber, N. & Sarmiento, J. L. Global patterns of marine nitrogen fixation and denitrification. *Global Biogeochem. Cycles* **11**, 235–266 (1997).
- Michaels, A. F. et al. Inputs, losses and transformations of nitrogen and phosphorus in the pelagic North Atlantic Ocean. *Biogeochemistry* **35**, 181–226 (1996).
- Lipschultz, F. & Owens, N. J. P. An assessment of nitrogen fixation as a source of nitrogen to the North Atlantic Ocean. *Biogeochemistry* **35**, 261–274 (1996).
- Zehr, J. P., Mellon, M. T. & Zani, S. New nitrogen fixing microorganisms detected in oligotrophic oceans by the amplification of nitrogenase (*nifH*) genes. *Appl. Environ. Microbiol.* **64**, 3444–3450 (1998).
- Zehr, J. P., Carpenter, E. J. & Villareal, T. A. New perspectives on nitrogen-fixing microorganisms in tropical and subtropical oceans. *Trends Microbiol.* **8**, 68–73 (2000).
- Chen, Y.-B., Dominic, B., Mellon, M. T. & Zehr, J. P. Circadian rhythm of nitrogenase gene expression in the diazotrophic filamentous nonheterocystous cyanobacterium *Trichodesmium* sp. Strain IMS 101. *J. Bacteriol.* **180**, 3598–3605 (1998).
- Beja, O. et al. Bacterial rhodopsin: evidence for a new type of phototrophy in the sea. *Science* **289**, 1902–1906 (2000).
- Kolber, Z. S., Van Dover, C. L., Niederman, R. A. & Falkowski, P. G. Bacterial photosynthesis in surface waters of the open ocean. *Nature* **407**, 177–179 (2000).
- Reddy, K. J., Haskell, J. B., Sherman, D. M. & Sherman, L. A. Unicellular, aerobic nitrogen-fixing cyanobacteria of the genus *Cyanothece*. *J. Bacteriol.* **175**, 1284–1292 (1993).
- Waterbury, J. B. & Rippka, R. in *Bergey's Manual of Systematic Bacteriology* Vol. 3 (ed. Staley, J. T.) 1728–1746 (Williams & Wilkins, Baltimore, 1989).
- Neveux, J., Lantoin, F., Vaulot, D., Marie, D. & Blanchot, J. Phycoerythrins in the southern tropical and equatorial Pacific Ocean: evidence for new cyanobacterial types. *J. Geophys. Res.* **104**, 3311–3321 (1999).
- Campbell, L., Liu, H., Nolla, H. A. & Vaulot, D. Annual variability of phytoplankton and bacteria in the subtropical North Pacific Ocean at station ALOHA during the 1991–1994 ENSO event. *Deep-Sea Res.* **44**, 167–192 (1997).
- Brass, S. et al. Utilization of light for nitrogen fixation by a new *Synechocystis* strain is extended by its low photosynthetic efficiency. *Appl. Environ. Microbiol.* **60**, 2575–2583 (1994).
- Wasmund, N., Voss, M. & Lochte, K. Evidence of nitrogen fixation by non-heterocystous cyanobacteria in the Baltic Sea and re-calculation of a budget of nitrogen fixation. *Mar. Ecol. Progr. Ser.* **214**, 1–14 (2001).
- Letelier, R. M. & Karl, D. M. Role of *Trichodesmium* spp. in the productivity of the subtropical North Pacific Ocean. *Mar. Ecol. Progr. Ser.* **133**, 263–273 (1996).
- Lin, S., Henze, S. & Carpenter, E. J. Whole-cell immunolocalization of nitrogenase in marine diazotrophic cyanobacteria, *Trichodesmium* spp. *Appl. Environ. Microbiol.* **64**, 3052–3058 (1998).

- Karl, D. et al. The role of nitrogen fixation in biogeochemical cycling in the subtropical North Pacific Ocean. *Nature* **388**, 533–538 (1997).
- Letelier, R. M. et al. Temporal variability of phytoplankton community structure based on pigment analysis. *Limnol. Oceanogr.* **38**, 1420–1437 (1993).
- Hawser, S. P., O'Neil, J. M., Roman, M. R. & Codd, G. A. Toxicity of blooms of the cyanobacterium *Trichodesmium* to zooplankton. *J. Appl. Phys.* **4**, 79–86 (1992).
- Karl, D. Comment: a new source of 'new' nitrogen in the sea. *Trends Microbiol.* **8**, 301 (2000).
- Zani, S., Mellon, M. T., Collier, J. L. & Zehr, J. P. Expression of *nifH* genes in natural microbial assemblages in Lake George, NY detected with RT-PCR. *Appl. Environ. Microbiol.* **66**, 3119–3124 (2000).
- Van de Peer, Y. & De Wachter, R. TREECON for Windows: a software package for the construction and drawing of evolutionary trees for the Microsoft Windows environment. *Comput. Applic. Biosci.* **10**, 569–570 (1994).

Acknowledgements

We thank the crews and participants of the HOT programme, especially L. Tupas and J. Dore for field support. We also thank L. Campbell for providing flow cytometer data. This work was supported by NSF Division of Ocean Sciences grants to J.P.Z., J.P.M. and D.M.K.

Correspondence and requests for materials should be addressed to J.P.Z. (e-mail: zehrj@cats.ucsc.edu).

Density-dependent mortality in an oceanic copepod population

M. D. Ohman*† & H.-J. Hirche‡

* Station Zoologique, 06230 Villefranche-sur-Mer, France

‡ Alfred Wegener Institute for Polar and Marine Research, D-27568 Bremerhaven, Germany

Planktonic copepods are primary consumers in the ocean and are perhaps the most numerous metazoans on earth. Secondary production by these zooplankton supports most food webs of the open sea, directly affecting pelagic fish populations and the biological pump of carbon into the deep ocean. Models of marine ecosystems are quite sensitive to the formulation of the term for zooplankton mortality^{1–4}, although there are few data available to constrain mortality rates in such models. Here we present the first evidence for nonlinear, density-dependent mortality rates of open-ocean zooplankton. A high-frequency time series reveals that per capita mortality rates of eggs of *Calanus finmarchicus* Gunnerus are a function of the abundance of adult females and juveniles. The temporal dynamics of zooplankton populations can be influenced as much by time-dependent mortality rates as by variations in 'bottom up' forcing. The functional form and rates chosen for zooplankton mortality in ecosystem models can alter the balance of pelagic ecosystems^{1–3}, modify elemental fluxes into the ocean's interior⁵, and modulate interannual variability in pelagic ecosystems⁶.

The high-frequency (sampling interval 1–2 d, sustained for 80 d) time series of *Calanus finmarchicus* in the central Norwegian Sea conducted as part of the TASC (Trans-Atlantic Study of *Calanus finmarchicus*) programme shows a springtime emergence of juvenile (C5) and adult female copepods in late March (small hump at front left of Fig. 1). These individuals originate from the overwintering generation in deep water⁷. The onset of reproductive maturity and egg production occur at least 40–50 d before the phytoplankton bloom^{8,9}, contrary to the assumptions in many ecosystem models, although per capita rates of egg production increase at the time of

† Present address: Scripps Institution of Oceanography, University of California, San Diego, La Jolla, California 92093-0218, USA.

the bloom⁹. Grazing rates by *C. finmarchicus* are low before the bloom^{10,11}, suggesting that stored wax esters are used during gonad maturation and oogenesis with nutritional supplements obtained from microplankton grazed from the water column. The recruitment rate (R_e ; number of eggs produced per m^2 of sea surface per d) is initially quite high, but for the first 20 d of the series virtually no eggs survive to the first larval stage (the nauplius). Subsequently, nauplius larvae appear and the population increases as a developing spring generation, which is apparent as a dark diagonal band across Fig. 1.

Stage-specific mortality rates from this series were estimated using inverse methods^{12,13} (see Fig. 2 legend and Methods for details). The high rates of instantaneous egg mortality (median = $1.76 d^{-1}$, equivalent to $82.8\% d^{-1}$) indicate that on average only 2.7% of eggs in this population survive to the first larval stage. The median rate of egg death is balanced by the median instantaneous birth rate ($1.71 d^{-1}$), but this seasonally averaged equilibrium masks the important temporal dynamics in the population. Rates of instantaneous egg mortality vary considerably with time. They peak on day 94–95, generally decline until day 129, then increase slowly after this period (Fig. 2a). Temporal variations in rates of egg mortality are greater than variations in birth rate (Fig. 2b).

Such losses cannot be attributed to advection alone. The sustained lack of nauplii for nearly 20 d—when eggs hatch in 2.16 d at

the ambient temperature of $6.4^\circ C$ (ref. 14)—implies that eggs perish consistently in upstream waters as well as at Ocean Station M. The residence time of a parcel of water equivalent to the dimensions of a 20-km *Calanus* patch¹⁵ can be estimated at 5 d from the mean springtime current speeds in the upper 100 m at Ocean Station M¹⁶. This residence time gives an average fractional daily loss due to advection of $20\% d^{-1}$, while the average rate of egg mortality is four times greater ($83\% d^{-1}$). A third line of evidence indicating that we have sampled the same planktonic population is the agreement between seasonally averaged rates of birth and mortality.

The highest rates of egg mortality occur at a time of very low diatom concentrations^{10,11} and thus are not consistent with deleterious effects of diatom metabolites¹⁷. Using fucoxanthin pigments as a measure of the biomass of diatoms¹¹, rates of *C. finmarchicus* egg mortality were not correlated with the concentration of diatoms in the water column ($P > 0.10$, Spearman's rank correlation, $n = 20$) or with the rate of ingestion of diatoms by *C. finmarchicus* adult females ($P > 0.10$, $n = 19$). The highest rates of egg mortality occur when adult males are most abundant¹⁸, when the adult male : female sex ratio is high (approximately 1 : 2)⁹, when immature females are relatively rare⁹, and when adult females all have full seminal receptacles (H.-J.H., unpublished observations). Such observations suggest that fertilization success is unlikely to account for high rates

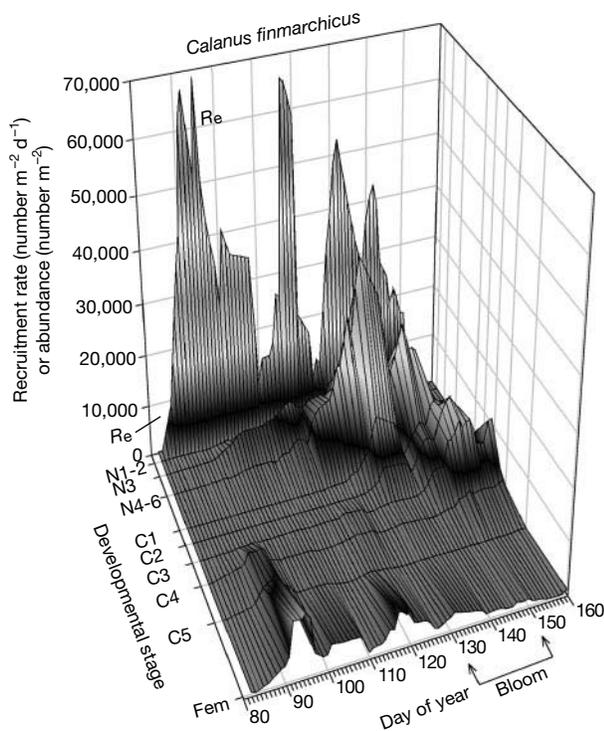


Figure 1 Spring population growth of the copepod *Calanus finmarchicus* at ocean station M, in the Norwegian Sea (centred on $66^\circ N$, $2^\circ E$). Bloom indicates the period of the phytoplankton bloom (maximum concentration 3 ng chlorophyll *a* per ml), which coincided with the onset of thermal stratification (see ref. 10). Pre-bloom concentrations were < 0.5 ng chlorophyll *a* per ml and post-bloom averaged 1.5 ng chlorophyll *a* per ml (ref. 10). The population was sampled with a 53- μm mesh WP2 net, towed vertically from 100 to 0 m, every 1–2 d from 22 March to 9 June 1997 (day of year 81–160). Daily rates of egg production were determined from 50 freshly collected individual females incubated aboard ship⁹, multiplied by the abundance of adult females to obtain the daily rate of egg recruitment (R_e ; eggs $m^{-2} d^{-1}$). Other values are abundances (number m^{-2}) of the following developmental stages: nauplius stages 1 and 2 combined (N1–2), N3, nauplius 4–6 combined (N4–6), copepodid stages C1 through to C5, and adult females (for details see refs 9 and 18). The raw data (see ref. 18) were smoothed with a four-point running mean and interpolated to a rectangular grid for plotting.

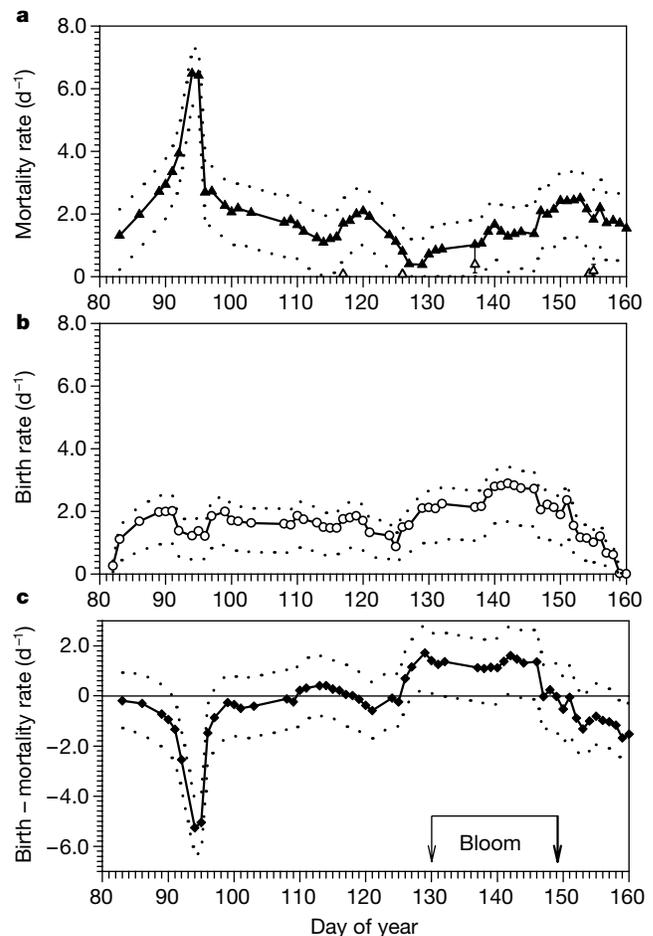


Figure 2 Instantaneous rates of egg mortality (a) ($m_e; d^{-1}$), birth (b) ($b; d^{-1}$) and their difference (c) ($b - m_e$) at ocean station M, with estimated 95% confidence intervals (dotted lines). Filled triangles in panel a show total egg mortality; open triangles show mortality attributable to egg-hatching success ($\bar{x} \pm 95\%$). Birth rates were obtained from $b = \ln(1 + R_e/2N_f)$, where R_e is rate of egg recruitment (eggs $m^{-2} d^{-1}$) and N_f is the number of adult females, assuming that the egg sex ratio was 1 : 1. See Methods for the calculation of embryonic mortality.

of egg mortality. If egg mortality were caused by a deficiency in micronutrients that are essential for embryonic development, this deficiency would be expected to diminish when food concentrations increase. Instead, rates of egg mortality were independent of the biomass of ciliate prey, or phytoplankton, and of the two prey types combined ($P > 0.10$, data from ref. 10), although we cannot rule out micronutrient deficiency definitively. Experiments on egg-hatching success on five occasions showed that mortality attributable to the production of nonviable eggs was a small fraction (average 10.2%) of total egg mortality (Fig. 2a).

The temporal decline in egg mortality rate (Fig. 2a) parallels the decline in abundance of adult female and late-stage juvenile copepods (Fig. 1). We found variations in the rate of instantaneous egg mortality to be directly proportional to the abundance of adult female and juvenile *C. finmarchicus* (Fig. 3, $P < 0.001$). The instantaneous mortality rate represents the probability of mortality; where this probability changes as a function of population density, it introduces a nonlinear term into equations of population dynamics³. In contrast to rates of egg mortality, birth rates were independent of the abundance of adult female and juvenile *C. finmarchicus* ($P > 0.05$).

The most parsimonious explanation for the density-dependence of egg mortality seems to be egg cannibalism. Experiments have established that *C. finmarchicus* adult females and stage C5 juveniles ingest eggs of conspecifics (J. A. Runge, personal communication) and similarly sized microzooplankton^{10,19} with high clearance rates. Egg predation would be particularly important during the pre-bloom period when phytoplankton concentrations are low. Application of experimentally measured clearance rates to adult females and stage C5 juveniles of *C. finmarchicus* show that if the copepods encounter patches of eggs in high concentrations in thin layers, or if encounter rates between *Calanus* and eggs are increased by ambient turbulence²⁰, experimentally measured rates of cannibalism are typically sufficient to account for daily rates of egg loss from the water column. However, such calculations depend on the concentrations of eggs encountered by copepods in the water column at the microscale, a problem that merits future research. The residuals from the regression in Fig. 3 are not consistently negative during the

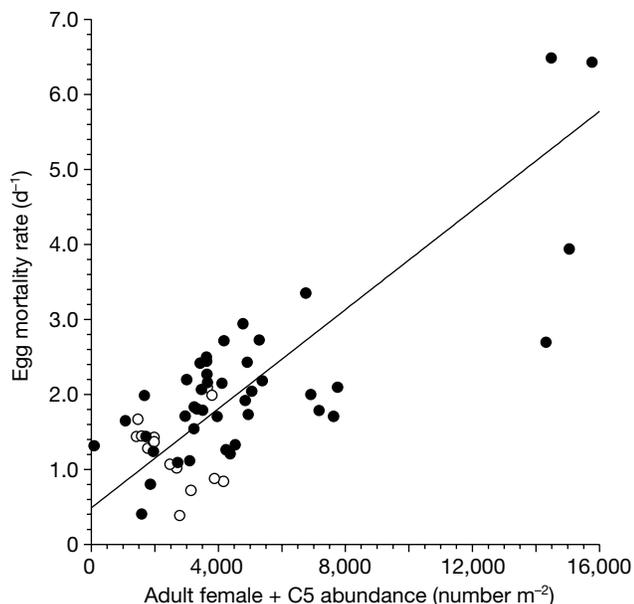


Figure 3 Dependence of embryonic mortality rates on the abundance of *Calanus finmarchicus* adult females and juvenile stage C5 at ocean station M. Filled symbols indicate the period before or after the phytoplankton bloom, open symbols the bloom period. The fitted line illustrates a model II functional regression, assuming error in both y and x values: $y = 0.00033x + 0.488$ ($r^2 = 0.608$, $P < 0.0001$).

spring bloom, as would be expected if the copepods were switching (see ref. 21) to alternative prey during the bloom. Although copepod egg cannibalism has been shown in laboratory containers and cannibalism has been inferred for natural copepod populations in semi-closed coastal environments^{22–24} and shallow continental shelf localities^{25,26}, this seems to be the first such suggestion for a zooplankton population of the open sea.

Why does reproduction persist early in the year if egg survivorship is so low? There is substantial interannual variability in the population size of *C. finmarchicus* in the North Atlantic²⁷. If cannibalism were the dominant mechanism explaining early egg mortality, year-to-year differences in the abundance of *Calanus* females would result in year-to-year differences in numbers of eggs surviving. An occasional year with low egg mortality would be sufficient to maintain the trait of early reproduction in the population.

The difference between birth and mortality rates ($b - m_e$) becomes approximately equal to 0 at day 100 (Fig. 2c), at which time the population begins increasing (Fig. 1). Although b subsequently increases at the time of the spring bloom (after day 130, Fig. 2b), the increase is preceded by an 8–10-d decline in egg mortality (Fig. 2a), which seems to initiate increased population growth shortly before the bloom (Fig. 2c). Thus the onset of net population growth seems to be affected at least as much, if not more, by changes in the rate of egg death as by variations in birth rate.

Traditional models of marine ecosystems emphasize the physical and biological processes influencing nutrient supply, dynamics of the phytoplankton spring bloom, and zooplankton grazing, on the assumption that this bottom-up perspective will predict the fecundity and production of marine zooplankton populations. Rates of zooplankton loss are often treated as constant and linear^{28,29}. The present results show that temporal variations of mortality rates, perhaps more than fecundity responses to a spring bloom, are of central importance in explaining the temporal variability of the dominant oceanic zooplankton in the North Atlantic. Mortality acting in a density-dependent manner can introduce self-limitation of some zooplankton populations of the open sea. Predictions of long-term variability in pelagic ecosystems cannot rely on only changes in ocean mixing and circulation^{27,28,30} but must also consider internal nonlinearities operating within pelagic populations. □

Methods

Embryonic mortality rates as a function of time

The calculation of the rates of embryonic mortality as a function of time ($m_e(t)$) (used to generate Fig. 2) were derived from a new solution to equations (5) and (11) of ref. 13:

$$m_e(t) = \frac{-\ln\left(\frac{N_{n1}(t)m_{n1}(t)}{R_e(t - a_e(t))(1 - e^{-m_{n1}(t)a_{n1}(t)})}\right)}{a_e(t)}$$

where $N_{n1}(t)$ is the abundance of the combined nauplius stage 1–2 at time t ; $m_{n1}(t)$ is the mortality rate of nauplius stage 1–2 at time t ; $R_e(t - a_e(t))$ is the rate of egg recruitment at time $t - a_e(t)$; and $a_e(t)$ is the embryonic duration at time t . This solution assumes that temperature-dependent embryonic duration changes slowly with time (that is, $da_e/dt \approx 0$), as confirmed from field measurements of temperature, and that R_e and m_{n1} are constant for the duration of the nauplius stages N1–2, $a_{n1}(t)$. The value for $m_{n1}(t)$ was obtained using Wood’s population surface method¹². The durations for eggs and naupliar stages N1–2 were obtained from Belehrádek functions¹⁴, using the average temperature in the upper 100 m of the water column. As all of these developmental stages are before feeding, their rate of development is controlled by ambient temperature.

Confidence intervals were estimated using 10,000 iterations of a parametric bootstrap procedure assuming that the error in N_{n1} was normally distributed on a log scale with a coefficient of variation of 70%; that other variables had normally distributed errors with coefficients of variation of $R_e = 70\%$, $m_{n1} = 50\%$, and $R_e/N_e = 40\%$, respectively; and that a_e and a_{n1} were known parameters.

Mortality at egg hatching was determined by counting the number of nauplii hatched from lots of 30–60 eggs over an interval of 3 d ($n = 6$ to 12 replicates per treatment), and expressed as an instantaneous coefficient ($-\ln(L_x/a_e)$), where L_x is the proportion of eggs surviving and a_e is the temperature-dependent embryonic duration. Egg-hatching data were supplied by U. Klenke.

Received 4 January; accepted 20 June 2001.

1. Steele, J. H. & Henderson, E. W. The role of predation in plankton models. *J. Plank. Res.* **14**, 157–172 (1992).
2. Fasham, M. J. R. Variation in the seasonal cycle of biological production in subarctic oceans: a model sensitivity analysis. *Deep-Sea Res.* **42**, 1111–1149 (1995).
3. Edwards, A. M. & Yool, A. The role of higher predation in plankton population models. *J. Plank. Res.* **22**, 1085–1112 (2000).
4. Carlotti, F., Giske, J. & Werner, F. *Zooplankton Methodology Manual* (eds Harris, R. P., Wiebe, P. H., Lenz, J., Skjoldal, H. R. & Huntley, M.) 571–667 (Academic, San Diego, 2000).
5. Fasham, M. J. R. *The Global Carbon Cycle* (ed. Heinemann, M.) 457–504 (Springer, New York, 1993).
6. Li, M., Gargett, A. & Denman, K. What determines seasonal and interannual variability of phytoplankton and zooplankton in strongly estuarine systems? Application to the semi-enclosed estuary of Strait of Georgia and Juan de Fuca Strait. *Estuar. Coast. Shelf Sci.* **50**, 467–488 (2000).
7. Heath, M. R. The ascent migration of *Calanus finmarchicus* from overwintering depths in the Faroe–Shetland Channel. *Fish. Oceanogr.* (Suppl. 1) **8**, 84–99 (1999).
8. Richardson, K., Jonasdottir, S. H., Hay, S. J. & Christoffersen, A. *Calanus finmarchicus* egg production and food availability in the Faroe–Shetland channel and northern North Sea: October–March. *Fish. Oceanogr.* (Suppl. 1) **8**, 153–162 (1999).
9. Niehoff, B. et al. A high frequency time series at Weathership M, Norwegian Sea, during the 1997 spring bloom: the reproductive biology of *Calanus finmarchicus*. *Mar. Ecol. Prog. Ser.* **176**, 81–91 (1999).
10. Irigoien, X. et al. A high frequency time series at weathership M, Norwegian Sea, during the 1997 spring bloom: feeding of adult female *Calanus finmarchicus*. *Mar. Ecol. Prog. Ser.* **172**, 127–137 (1998).
11. Meyer-Harms, B., Irigoien, X., Head, R. & Harris, R. Selective feeding on natural phytoplankton by *Calanus finmarchicus* before, during, and after the 1997 spring bloom in the Norwegian sea. *Limnol. Oceanogr.* **44**, 154–165 (1999).
12. Wood, S. N. Obtaining birth and mortality patterns from structured population trajectories. *Ecol. Monogr.* **64**, 23–44 (1994).
13. Aksnes, D. L., Miller, C. B., Ohman, M. D. & Wood, S. N. Estimation techniques used in studies of copepod population dynamics—a review of underlying assumptions. *Sarsia* **82**, 279–296 (1997).
14. Campbell, R. G., Wagner, M. M., Teegarden, G. J., Boudreau, C. A. & Durbin, E. G. Growth and development rates of the copepod *Calanus finmarchicus* reared in the laboratory. *Mar. Ecol. Prog. Ser.* (in the press).
15. Solow, A. R. & Steele, J. H. Scales of plankton patchiness: biomass versus demography. *J. Plank. Res.* **17**, 1669–1677 (1995).
16. Hainbucher, D. & Backhaus, J. O. Circulation of the eastern North Atlantic and north-west European continental shelf—a hydrodynamic modelling study. *Fish. Oceanogr.* (Suppl. 1) **8**, 1–12 (1999).
17. Miralto, A. et al. The insidious effect of diatoms on copepod reproduction. *Nature* **402**, 173–176 (1999).
18. Hirche, H.-J., Brey, T. & Niehoff, B. A high frequency time series at Weathership M, Norwegian Sea: population dynamics of *Calanus finmarchicus*. *Mar. Ecol. Prog. Ser.* (in the press).
19. Ohman, M. D. & Runge, J. A. Sustained fecundity when phytoplankton resources are in short supply: omnivory by *Calanus finmarchicus* in the Gulf of St. Lawrence. *Limnol. Oceanogr.* **39**, 21–36 (1994).
20. Rothschild, B. J. & Osborn, T. R. Small-scale turbulence and plankton contact rates. *J. Plank. Res.* **10**, 465–474 (1988).
21. Landry, M. R. Switching between herbivory and carnivory by the planktonic marine copepod *Calanus pacificus*. *Mar. Biol.* **65**, 77–82 (1981).
22. Landry, M. R. Population dynamics and production of a planktonic marine copepod, *Acartia clausii*, in a small temperate lagoon on an Juan Island, Washington. *Int. Rev. Ges. Hydrobiol.* **63**, 77–119 (1978).
23. Uye, S. I. & Liang, D. Copepods attain high abundance, biomass and production in the absence of large predators but suffer cannibalistic loss. *J. Mar. Sys.* **15**, 495–501 (1998).
24. Peterson, W. T. & Kimmerer, W. J. Processes controlling recruitment of the marine calanoid copepod *Temora longicornis* in Long Island Sound: egg production, egg mortality, and cohort survival rates. *Limnol. Oceanogr.* **39**, 1594–1605 (1994).
25. Daan, R., Gonzales, S. R. & Klein Breteler, W. C. M. Cannibalism in omnivorous calanoid copepods. *Mar. Ecol. Prog. Ser.* **47**, 45–54 (1989).
26. Ohman, M. D., Durbin, E. G. & Runge, J. A. Density-dependence of instantaneous mortality rates of *Calanus finmarchicus* on Georges Bank. *EOS Trans. Am. Geophys. Union* **79**, OS155 (1998).
27. Planque, B. & Taylor, A. H. Long-term changes in zooplankton and the climate of the North Atlantic. *ICES J. Mar. Sci.* **55**, 644–654 (1998).
28. Lynch, D. R., Gentleman, W. C., McGillicuddy, D. J. Jr & Davis, C. S. Biological/physical simulations of *Calanus finmarchicus* population dynamics in the Gulf of Maine. *Mar. Ecol. Prog. Ser.* **169**, 189–210 (1998).
29. Cowan, R. K., Lwiza, K. M. M., Sponaugle, S., Paris, C. B. & Olson, D. B. Connectivity of marine populations: open or closed? *Science* **287**, 857–859 (2000).
30. Heath, M. R. et al. Climate fluctuations and the spring invasion of the North Sea by *Calanus finmarchicus*. *Fish. Oceanogr.* (Suppl. 1) **8**, 163–176 (1999).

Acknowledgements

We thank the late M. M. Mullin for his scientific insights, the captain and the crew as well as the scientists (X. Irigoien, U. Klenke, R. Head) on the vessel *Polarfront* for their support, and the Institute for Marine Research (Bergen, Norway), which provided logistical help. B. Niehoff provided egg-production rates, S. Jaklin and E. Mizdalski helped with analysing the samples and A. De Robertis generated bootstrap confidence intervals. This work was supported by funding from the European Commission through the TASC project and by the National Science Foundation and the National Oceanic and Atmospheric Administration through US GLOBEC (Global Ocean Ecosystem Dynamics).

Correspondence and requests for materials should be addressed to M.D.O. (e-mail: mohman@ucsd.edu).

Erythropoietin-mediated neuroprotection involves cross-talk between Jak2 and NF-κB signalling cascades

Murat Digicaylioglu & Stuart A. Lipton

Center for Neuroscience and Aging Research, The Burnham Institute, 10901 North Torrey Pines Road, La Jolla, California 92037, USA
Cerebrovascular and Neuroscience Research Institute, Brigham and Women's Hospital, Program in Neuroscience, Harvard Medical School, Boston, Massachusetts 02115, USA

Erythropoietin, a kidney cytokine regulating haematopoiesis (the production of blood cells), is also produced in the brain after oxidative or nitrosative stress^{1,2}. The transcription factor hypoxia-inducible factor-1 (HIF-1) upregulates EPO following hypoxic stimuli^{3,4}. Here we show that preconditioning with EPO protects neurons in models of ischaemic and degenerative damage due to excitotoxins^{4,5} and consequent generation of free radicals, including nitric oxide (NO). Activation of neuronal EPO receptors

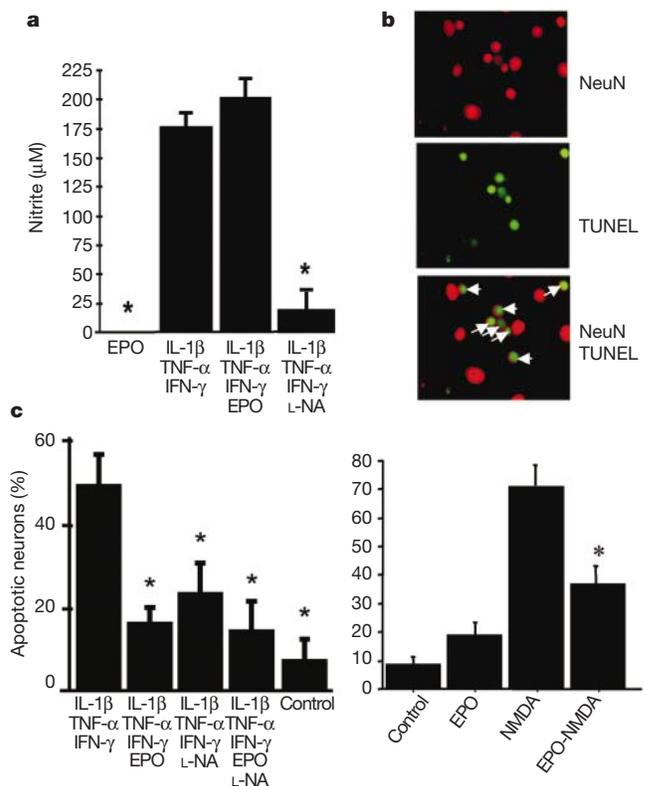


Figure 1 Neuroprotective effect of EPOR activation on cerebrocortical neurons. **a**, Incubation of rat cerebrocortical cultures for 6 h with cytokines (IFN-γ, 500 U ml⁻¹; TNF-α, 200 U ml⁻¹; IL-1β, 5 ng ml⁻¹) increased NO, as reflected by nitrite concentration. EPO (5 U ml⁻¹) did not affect nitrites, whereas L-nitroarginine (L-NA; 1 mM) dramatically reduced nitrite production; asterisk, P < 0.001 by analysis of variance (ANOVA). **b**, Apoptotic neurons (arrows) identified by labelling with both anti-NeuN (red) and TUNEL (green). **c**, Neuronal apoptosis increased after NMDA (300 µM) or cytokine-induced NO production, but decreased with EPO. Pre-incubation with EPO (5 U ml⁻¹, 3 h) dramatically decreased the number of apoptotic neurons (asterisk, P < 0.001). L-nitroarginine (1 mM) administered with cytokines also decreased the number of apoptotic neurons.